MRS Advances © 2016 Materials Research Society
DOI: 10.1557/adv.2016.172

Investigation of GaSb/GaAs Quantum Dots Formation on Ge (001) Substrate and Effect of Anti-Phase Domains

Zon[1], Thanavorn Poempool[1], Suwit Kiravittaya[2], Suwat Sopitpan[3], Supachok Thainoi[1], Songphol Kanjanachuchai[1], Somchai Ratanathammaphan[1] and Somsak Panyakeow[1]

[1]Semiconductor Device Research Laboratory (SDRL), Department of Electrical Engineering, Faculty of Engineering, Chulalongkorn University, Bangkok, 10330, Thailand
[2]Department of Electrical and Computer Engineering, Faculty of Engineering, Naresuan University, Phitsanulok, Thailand
[3]Thailand Microelectronic Center (TMEC), National Science and Technology Agency (NSTDA), Chachoensao, Thailand

ABSTRACT

The effects of GaAs anti-phase domains (APDs) on the growth of GaSb quantum dots (QDs) are investigated by molecular beam epitaxial growth of GaAs on Ge (001) substrate. Ge is a group-IV element and GaAs is a polar III-V compound semiconductor. Due to polar/non polar interface, GaAs APDs are formed. Initial formation of APD relates to a non-uniform growth of high index GaAs surfaces. However, due to high sticking coefficient of Sb atoms at low substrate growth temperature, GaSb QDs can be formed on the whole surface of the sample without any effects from APD boundary. The buffer layer growth temperature is one of the key roles to control the APDs formation. Therefore we tried to adjust the optimum conditions such as buffer layer thickness and growth temperature to get nearly flat sample surface with large APDs for high QDs density (~ 8×10^9 dots/cm^2). Low-temperature photoluminescence is conducted and GaSb QDs peak is observed at the energy range of 1.0 eV-1.3 eV.

INTRODUCTION

GaSb/GaAs quantum dot (QD) has the staggered type-II band alignment, which is attractive in many aspects. In staggered type-II band alignment, the conduction band and valence band of GaSb QDs have higher energy level than those of the GaAs matrix. Therefore excited/injected electrons will locate in GaAs matrix around GaSb QDs by Coulomb attraction and holes will be confined in GaSb QDs. The electron and hole wave-functions are spatial separated and give a long carrier lifetime, which might be useful for memory devices and high-operating-temperature infrared photodetectors [1-3]. High density type II GaSb/GaAs QDs are also promising nanostructure for intermediate band solar cells and IR detectors [4, 5]. Combination of this type II GaSb/GaAs and Ge can give extended spectral responses of the devices. The band gap properties of GaAs and Ge, i.e., direct/indirect and wide/narrow bandgaps, are applicable for many optoelectronic devices. Small lattice mismatch between GaAs buffer layer and Ge substrate, which is only 0.1%, allows us to realize defect-free

heterostructure. However, growing of polar semiconductor (GaAs) on non-polar semiconductor (Ge) creates anti-phase domains (APDs). APD boundary is considered as defects which are undesirable for device performance. It is curious to investigate the effect of APDs on physical, electrical and optical properties of GaSb/GaAs nanostructure on Ge.

In this research, two samples (S2, S3); one (S2) with 1.4 monolayer (ML)-one layer of GaSb/GaAs QDs layer and another (S3) with 2 & 3 ML-two layers of QDs are grown on Ge (001) substrate for comparison by solid-source molecular beam epitaxy (MBE). QDs are self-assembled by Stranski-Krastanov mode due to 7% lattice mismatch between GaSb and GaAs [6].It is also found that GaAs APDs do not affect significantly on position of GaSb/GaAs QDs when the GaAs buffer layer is thick enough. However, the QDs formation depends on dots growth temperature. The noticeable research highlight is to describe the reliable results of growing the GaSb/GaAs QDs on conventional (001) Ge substrate although misoriented Ge substrate such as 6º miscut Ge substrate can be used to supress APDs formation [7, 8].

EXPERIMENTAL PROCEDURE

GaSb/GaAs QDs were grown on Ge (001) substrate by using MBE Compact 21 with Sb valved cracker. The elemental sources of Sb, Ga and As were used for growth procedure. At first Ge (001) substrates were preheated in preheating chamber to remove the surface contaminations. Before growth, Ge substrate was deoxidized by increasing the annealing temperature up to 540ºC in As_4 atmosphere. We investigated the deoxidizing temperature of substrate by checking reflection high-electron energy diffraction (RHEED) pattern. For all three samples (S1, S2 & S3), although deoxidizing temperatures for Ge substrates were slightly different, the average deoxidizing temperature is ~500ºC. The V/III flux ratio for GaAs buffer layer was adjusted to 13 for growth rate ~ 0.5 ML/s and ratio 4 for GaSb QDs growth to get growth rate ~ 0.14 ML/s for all samples. For the sample (S1), only GaAs buffer layer of about 50 nm was grown at deoxidizing temperature ~515ºC to study APDs formation on Ge substrate. In the second (S2) and the third (S3) samples, GaSb/GaAs QDs were grown by changing the GaAs buffer layer thickness, buffer growth temperature and QDs growth temperature to compare the QDs formation.

For the second (S2) sample, 600-nm-thick GaAs buffer layer was grown in two steps (two layers; 300 nm each) separately prior to the GaSb QDs. First 300-nm buffer layer was grown at the substrate deoxidizing temperature (515ºC). Second 300-nm layer was grown at 550ºC. After buffer layer growth, substrate temperature was ramped down to QDs growth temperature (450ºC) and ramped down the As cell temperature to 100ºC to reduce the background pressure to below $5x10^{-9}$ torr for sure to grow next step GaSb QDs layer. Arsenic cell shutter was closed when the cell temperature reached 200ºC. After arriving the QDs growth background pressure, 1.4 ML GaSb QDs were grown with V/III flux ratio 4 at growth temperature 450ºC which is ~100ºC lower than the second GaAs buffer layer growth temperature for cooling down the substrate temperature to grow QDs.

For the third sample (S3), we changed the buffer layer growth temperature to 500ºC for both steps (250-250 nm) because the substrate deoxidization happened at ~500ºC in this time, and the (2×2)-to-*c*(4×4) RHEED transition temperature was 457ºC respectively. This time 3ML QDs were grown initially at 407ºC which is 50ºC less than transition temperature while QDs in second sample (S2) was grown at transition temperature. Then GaAs cap layer was grown in two steps at 357ºC and 407ºC respectively for PL measurement, and 2ML QDs were proceeded at 407ºC for AFM analysis. We have done QDs growth at different temperatures to study the changing of QDs formation depends on temperature and buffer layers growth at different thickness in a little different of temperatures to investigate the APDs formation on Ge substrate.

The surface morphology such as APDs formation and GaSb/GaAs QDs nanostructure of the samples were characterized by atomic force microscopy (AFM Seiko SPA-400) in dynamic force mode. For PL study, 514.5-nm line Ar^+ laser is used for photo excitation. The power is varied from 40 mW to 200 mW and the measurement is performed at 20 K and 30 K.

RESULTS AND DISCUSSION

Figure 1(a) shows the 5×5 μm^2 AFM image of GaAs APDs formed on Ge (001) substrate (S1) with schematic diagram. Upper right image is the AFM image shown with surface slope scale. For 50 nm thick GaAs buffer layer, the size of APD is a quite small and the rough surface is formed. Figure 1(b) is the 3×3 μm^2 AFM image of GaSb/GaAs QDs (S2). At high QDs growth temperature (450ºC), QDs formed on only APD boundary (APB) and the dots density is low. When the QDs growth temperature is decreased to 407ºC, GaSb/GaAs QDs form on APDs and APBs (S3) with increasing dots density which is shown in figure 1(c). In all figures, their respective AFM images by surface slope scale and schematic diagrams are illustrated. Figure 1(a) was shown in large area for seeing clearly the nature of APDs in 50 nm thick buffer layer growth. In 3×3 μm^2 area of figure 1(b), we can investigate well both of APDs formation and QDs formation, and we maximized to 2×2 μm^2 for figure 1(c) to analyse the QDs formation in APDs and on APBs.

The surface orientation mapping, which is so-called facet-plot was analysed to quantify the QDs formulated on respective growth conditions, and also GaAs buffer layer growth [9]. Figure 2(a-c) shows the facet diagrams of three samples. GaAs crystallographic structure of GaAs buffer layer (S1) is shown in figure 2(a). Figure 2 (b & c) show the facet plots of GaSb/GaAs QDs on APBs (S2) and on both APBs and APDs (S3) respectively. When QDs were formed in high density, dots faceted plot showed the round base shape.

The formulated dots' heights and diameters at low QDs growth temperature was shown in figure 3. At high QDs growth temperature, the dots density is ~ 9×10^8 dots/cm^2 and at low temperature, the dots density is ~8×10^9dots/cm^2.

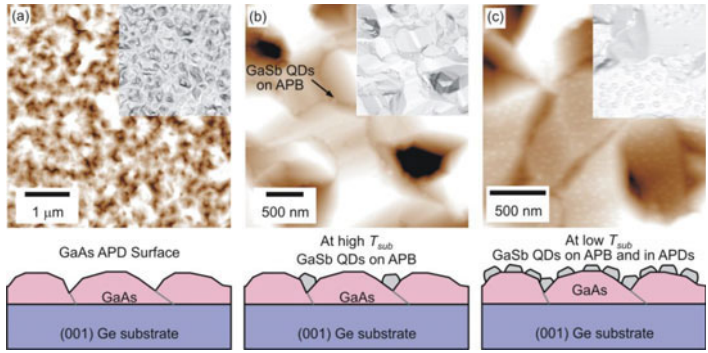

Figure 1.(a) 5×5 μm^2 AFM image of GaAs APDs, **(b)** 3×3 μm^2 AFM image of GaSb/GaAs QDs (1.4 ML) and **(c)** 2×2 μm^2 AFM image of GaSb/GaAs QDs (2 ML) on top formation on Ge (001) substrate with schematic diagrams. Upper right images are the AFM images with surface slope scale.

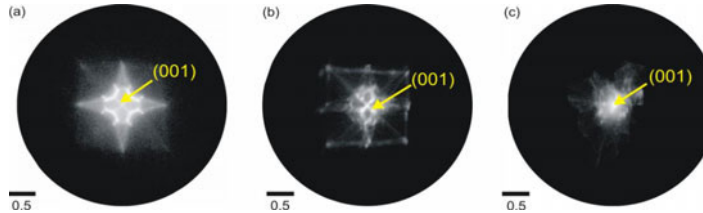

Figure 2. Facet plots of **(a)** GaAs crystallographic structure of GaAs buffer layer on Ge substrate (S1), **(b)** Low density GaSb/GaAs QDs formed on APBs at high QDs growth temperature (S2) and **(c)** high density GaSb/GaAs QDs formed on APDs and APBs at low QDs growth temperature (S3).

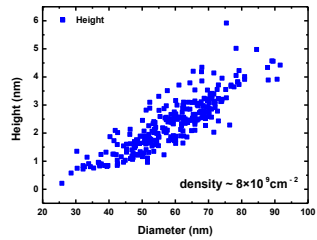

Figure 3. The dots height versus diameter for the low growth temperature grown QDs (S3).

At low QDs growth temperature (S3), high density QDs can be formed. Therefore, PL measurement was done by power dependence (40 mW to 200 mW) and temperature dependence at 20 K & 30 K as shown in figure 4 (a & b). In comparison of QDs peak position between 20 K and 30 K at 200 mW, the emission energy of QDs at 30 K shifts to lower energy (longer wavelength) and intensity is lower than that of 20 K. However, the intensity of QDs is getting higher than the GaAs layer starting from excitation power 144 mW and ahead.

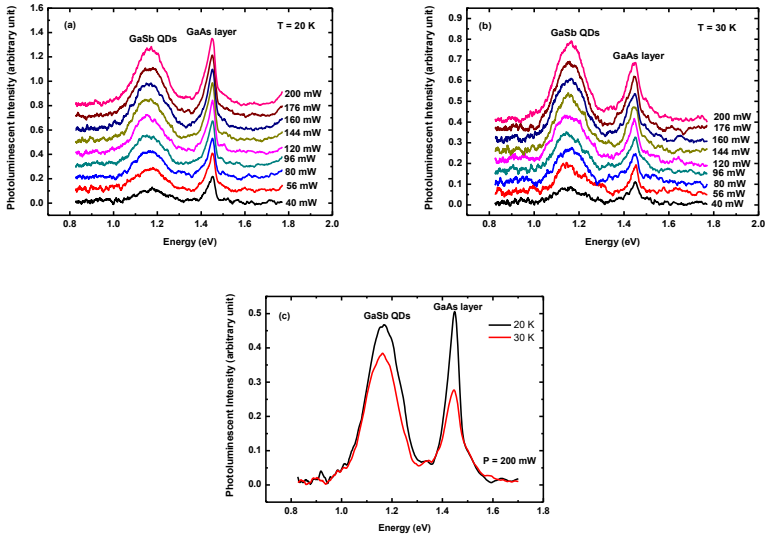

Figure 4. PL spectra obtained from GaSb/GaAs QDs in power dependence (40 mW to 200 mW) **(a)** at 20 K, **(b)** 30 K and **(c)** PL spectra of GaSb/GaAs QDs in temperature dependence (20 K & 30 K) at 200 mW for S3.

CONCLUSIONS

We fabricated three samples: one (S1) for investigation of APDs formation on Ge (001) substrate by growing of 50 nm thick GaAs buffer layer, other two samples (S2 & S3) for comparison of GaSb/GaAs QDs formation on APDs and APBs by changing the buffer layer thickness and QDs growth temperature. Low density QDs (9×10^8 dots/cm^2) are formed on APBs at high QDs growth temperature (450ºC) while high density QDs (8×10^9 dots/cm^2) are formed at low temperature (407ºC). The shape of QD at high density is almost round base shape and facet of the dots cannot be seen. From the PL measurement of S3, the emission peaks of QDs are wide from 1 eV to1.3 eV. PL peak energy redshifts when temperature is increased.

ACKNOWLEDGEMENTS

The authors would like to express appreciation for the supports of the Research Chair Grant, the National Science and Technology Development Agency (NSTDA), Thailand, Asian Office of Aerospace Research and Development (AOARD) [Contact No. FA2386-14-1-4081], Nanotechnology Centre of Thailand (NANOTEC), Thailand Research Fund (TRF) [Grant no. DPG 5380002], Chulalongkorn University, Research University Program of office of High Education Commission in Energy Cluster of Chulalongkorn University (EN264A) and ASEAN University Network/Southeast Asia Engineering Education Development Network (AUN/SEED-Net).

REFERENCES

1. C. K. Sun, G. Wang, J. E. Bowers, B. Brar, H. R. Blank, H. Kromer, and M. H. Pikuhn, Appl. Phys. Let. 68(11), 1543-1545 (1996).
2. T. Kawazu, T. Noda, T. Mano, Y. Sakuma, and H. Sakaki, Jpn. J. Appl. Phys. **54**, 04DH01 (2015).
3. C. Jiang, H. Sakaki, Physica E **32**, 17-20 (2006).
4. P. J. Carrington, A. S. Mahajumi, M. C. Wagener, J. R. Botha, Q. Zhuang, and A. Krier, Physica B **407**, 1493-1496 (2012).
5. P. D. Hodgson, R. J. Young, M. A. Kamarudin, P. J. Carrington, A. Krier, Q. D. Zhuang, E. P. Smakman, P. M. Koenraad, and M. Hayne, J. Appl. Phys. **114**, 073519 (2013).
6. M. Kunrugsa, S. Kiravittaya, S. Sopitpan, S. Ratanathammaphan, and S. Panyakeow, Journal of Crystal Growth **401**, 441-444 (2014).
7. Y. Li, G. Salviati, M. M. G. Bongers, L. Lazzarini, L. Nasi, L. J. Giling, Journal of Crystal Growth **163**, 195-202, (1996).
8. K. L. Schulte, A. W. Wood, R. C. Reedy, A. J. Ptak, N. T. Meyer, S. E. Babcock, and T. F. Kuech, J. Appl. Phys. **113**, 174903 (2013).
9. G. Costantini, A. Rastelli, C. Manzano, R. Songmuang, O. G. Schmidt, and K. Kern, H. V. Känel, Appl. Phys. Lett., **85** (23), 5673 (2004).